Available online at www.sciencedirect.com

ScienceDirect

Mendeleev Commun., 2023, **33**, 95–98

Mendeleev Communications

Molecular structure of 1,1′,6,6′-tetraaza-7,7′-bi(bicyclo[4.1.0]heptane) in gas, solid and solution phases: GED, XRD and NMR data combined with quantum chemical calculations

Alexander V. Belyakov,*[a] Vladimir V. Kuznetsov,[b] Galina S. Shimanskaya,[a] Anatoly N. Rykov,[c] Alexander S. Goloveshkin,[d] Yulia V. Novakovskaya[c] and Igor F. Shishkov*[c]

[a] *St. Petersburg State Institute of Technology (Technical University), 190013 St. Petersburg, Russian Federation. E-mail: belyakov@lti-gti.ru*
[b] *N. D. Zelinsky Institute of Organic Chemistry, Russian Academy of Sciences, 119991 Moscow, Russian Federation*
[c] *Department of Chemistry, M. V. Lomonosov Moscow State University, 119991 Moscow, Russian Federation. E-mail: ifshishkov@phys.chem.msu.ru*
[d] *A. N. Nesmeyanov Institute of Organoelement Compounds, Russian Academy of Sciences, 119991 Moscow, Russian Federation*

DOI: 10.1016/j.mencom.2023.01.030

The equilibrium molecular structure of 1,1′,6,6′-tetraaza-7,7′-bi(bicyclo[4.1.0]heptane) in the gas phase has been determined from the data of the gas phase electron diffraction method using quantum chemical calculations up to the RI-MP2/def2-QZVPP level of theory. Structure studies were also carried out in $CDCl_3$ solution using 1D and 2D ^1H and ^{13}C NMR spectroscopy and in the solid state using X-ray diffraction analysis. In the gas phase, three conformers of the molecule have been identified, while only one conformer is present in the $CDCl_3$ solution and in the solid state, in which the substance crystallizes in space group $P\bar{1}$.

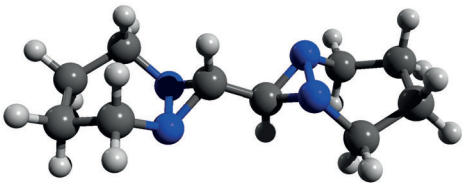

1,1′,6,6′-Tetraaza-7,7′-bi(bicyclo[4.1.0]heptane) molecular structure in gas, solid and solution

Keywords: 1,1′,6,6′-tetraaza-7,7′-bi(bicyclo[4.1.0]heptane), conformational analysis, gas and solid phases, $CDCl_3$ solution, GED, XRD, NMR, quantum chemical simulations.

The study of the molecular structure of diaziridines (1,2-diazacyclopropanes) has been an area of scientific interest for many years.[1–9] This class of compounds is of great theoretical and practical significance in different fields of science and engineering. In particular, diaziridine derivatives efficiently act on the central nervous system, exhibiting various types of neurotropic activity,[10–12] and the introduction of a second diaziridine cycle into the molecule increases activity.[10] Diaziridines are convenient objects for studying the stereochemistry of nitrogen due to the high stability of two stereogenic pyramidal nitrogen atoms.[13,14] The diaziridine ring is susceptible to ring-expansion reactions that result in the formation of a variety of five- to eight-membered mono- and bicyclic heterocyclic structures.[15–20] Important properties of diaziridines are high enthalpies of formation and low toxicity,[21] which make them potential promising components of liquid rocket propellants instead of toxic hydrazine derivatives. Therefore, the study of the properties of diaziridine derivatives of various structures remains highly relevant.

The study of the structure of 6-phenyl-1,5-diazabicyclo[3.1.0]-hexane[9] and 6-(4-chlorophenyl)-1,5-diazabicyclo[3.1.0]hexane (ClPh-DABHx)[2] using X-ray diffraction (XRD) analysis showed that the bicyclic fragment in these molecules has a flattened boat conformation. It was found that 1,1′,5,5′-tetraaza-6,6′-bi(bicyclo-[3.1.0]hexane) (bi-DABHx) has a boat conformation not only in a solid crystal,[1] but also in gas phase according to gas-phase electron diffraction (GED) data.[3] Additionally, XRD of 7-phenyl-1,6-diazabicyclo[4.1.0]heptane (Ph-DABHp)[2] and 7-(4-chlorophenyl)-1,6-diazabicyclo[4.1.0]heptane (ClPh-DABHp)[15] showed that the bicyclic hexahydropyridazine fragment of these molecules in the crystal has a chair conformation. In this work, for the first time, we succeeded in carrying out a GED study of the 1,6-diazabicyclo[4.1.0]heptane system by an example of 1,1′,6,6′-tetraaza-7,7′-bi(bicyclo[4.1.0]heptane) (bi-DABHp). Concurrently, this molecule was studied by XRD in a solid state and NMR spectroscopy in solution. Its expected energetically favorable configuration is shown in Figure 1 with the numbering of atoms used. From the point of view of structural chemistry, this is a non-rigid molecule with movements of moderate amplitude along several internal torsion coordinates. Note that two rotational movements relative to the flat diaziridine cycle are possible in the bi-DABHx molecule: turning of ethylene substituents around their bonds with the three-membered cycle, *i.e.*, around two N–C bonds.

A conformational analysis based on a series of quantum chemical calculations revealed the existence of six conformers **a**–**f** of the bi-DABHp molecule on the potential energy surface (Figure 2).

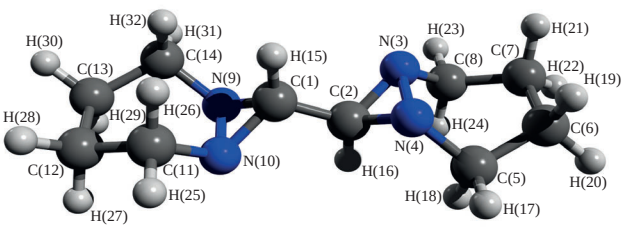

Figure 1 Molecular model of bi-DABHp.

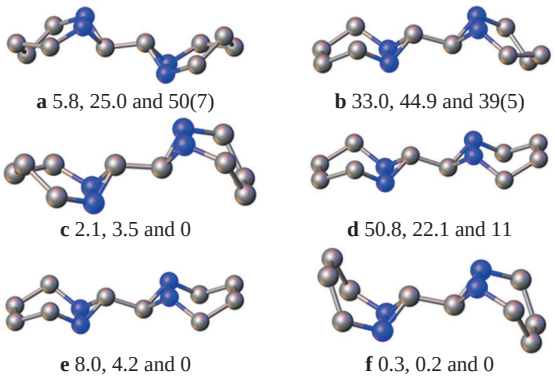

Figure 2 Conformations of the bi-DABHp molecule and their mole fractions (%) estimated at the RI-MP2, DFT-D3 and GED levels, respectively. The σ values of the least squares (LS) refinement are shown in parentheses.

Geometry optimization was performed at the all-electron second order Møller–Plesset perturbation theory level by the resolution-of-identity technique (RI-MP2) using the def2-QZVPP basis set (Table S3 in Online Supplementary Materials), as well as at the density functional level with the M062X-GD3 functional combined with Grimme's D3 dispersion correction (DFT-D3) using the aug-cc-pVTZ basis set (Table S4). The calculations were carried out with the Orca 4.2.0[22] and Gaussian 16 (Revision C.01)[23] program packages, respectively. In DFT-D3 simulations, normal coordinate analysis was used to prove the nature of stationary points on the potential energy surface and to calculate the thermodynamic functions of ensembles of different conformers under normal conditions. The resulting relative Gibbs energies were used to estimate the fractions of conformers in terms of the Boltzmann distribution at 298 K. These estimates (see Figure 2) are compared with similar estimates calculated from the total electronic energies of the same structures found at the RI-MP2 level and with estimates derived from the analysis of the GED data (Tables S1 and S2, Figures S2 and S3). It is worth noting that the fractions of conformers **b** and **d**, which are generally closest to spatial zigzags, are the largest, although the relative amount of these conformers differs significantly depending on the simulation level and thermal effects.

Mean vibrational amplitudes and vibrational corrections to internuclear distances (Tables S5–S7) required for the GED analysis

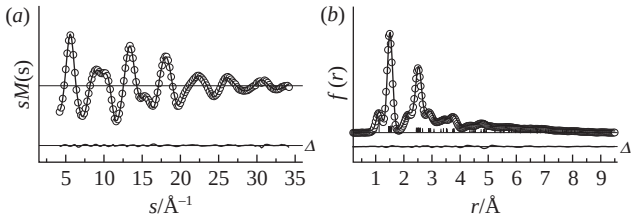

Figure 3 (*a*) Molecular intensity functions $sM(s)$ and (*b*) radial distribution functions $f(r)$ of the mixture of bi-DABHp conformers **a**, **b** and **d**. The experimental and calculated functions are shown by dotted and solid lines, respectively, and their difference functions (Δ) are also shown below them.

were computed using quadratic and cubic force fields, respectively, at the first-order perturbation theory level, taking into account curvilinear kinematic effects implemented in the SHRINK computer program.[24] These force fields were calculated at the DFT level with the B3LYP functional and the SNSD basis set.

To close the ring, the calculation of the Cartesian coordinates of atoms does not end at the last atom of the ring, but continues for three dummy atoms according to the same rules.[25] The problem of closing the ring is reduced to an iterative solution of nonlinear equations with respect to dependent geometrical parameters so that the Cartesian coordinates of dummy atoms coincide with the coordinates of first three atoms of the ring.

The structure was refined by the least squares method using a modified version of the KCED25 program.[26] The weight matrices were diagonal. The electron diffraction apparatus camera distance data (Table S1) were taken with weights of 0.5 and 1.0 for short and long camera distances, respectively.

The molecular geometry of bi-DABHp (see Figure 1) is determined by 18 internuclear distances, 34 valence bond angles and 33 dihedral angles. Among them, two internuclear distances, six bond angles and eight dihedral angles are ring closure parameters (Tables S8 and S9). Geometrical parameters and mean least-square vibrational amplitudes were refined in groups with constant differences from the theoretical MP2 and DFT-B3LYP estimates, respectively. In particular, the mean least-square amplitudes were refined in six groups according to the specific ranges of the radial distribution curve (Figure 3): 1.0−1.8, 1.8−2.8, 2.8−3.2, 3.2−4.1, 4.1−5.2 and 5.2−8.0 Å. The internuclear distances were refined in two groups, namely, the groups of C–H internuclear distances

Table 1 Main equilibrium structural parameters of bi-DABHp conformers.

Internuclear distances[a]/Å	Conformers			Bond angles[a]/deg	Conformers			Dihedral angles/deg	Conformers		
	a	**b**	**d**		**a**	**b**	**d**		**a**	**b**	**d**
C(1)–C(2)	1.472	1.472	1.471	C(1)–C(2)–N(3)	117.0	116.7	116.5	C(2)–N(3)–N(4)–C(5)	105.4	102.5	107.3
C(2)–N(3)	1.441	1.428	1.436	C(1)–C(2)–N(4)	116.7	117.0	116.5	C(6)–C(5)–N(4)–N(3)	–17.7	20.9	57.6
C(2)–N(4)	1.428	1.440	1.436	C(5)–N(4)–N(3)	118.7	118.6	111.9	C(7)–C(6)–C(5)–N(4)	48.8	–52.9	–56.9
N(3)–N(4)	1.510	1.510	1.519	C(6)–C(5)–N(4)	116.9	114.7	108.3	C(5)–C(6)–C(7)–C(8)[b]	–65.4	65.7	0.1
C(5)–N(4)	1.459	1.473	1.459	C(5)–C(6)–C(7)	107.9	109.2	110.8	C(6)–C(7)–C(8)–N(3)[b]	52.6	–48.7	56.7
C(5)–C(6)	1.514	1.510	1.517	C(6)–C(7)–C(8)[b]	109.2	107.9	110.8	C(7)–C(8)–N(3)–N(4)[b]	–20.7	17.6	–57.5
C(6)–C(7)	1.510	1.510	1.534	C(7)–C(8)–N(3)[b]	114.9	116.7	108.3	C(5)–N(4)–N(3)–C(8)[b]	2.8	–2.9	–0.1
C(7)–C(8)	1.510	1.514	1.517	C(8)–N(3)–N(4)[b]	118.6	118.9	112.1	N(3)–C(2)–C(1)–N(9)	107.8	107.7	107.6
C(8)–N(3)[b]	1.473	1.459	1.459	C(2)–C(1)–N(9)	116.7	116.5	116.5	C(1)–N(9)–N(10)–C(11)	102.5	107.3	107.3
C(1)–N(9)	1.428	1.437	1.436	C(2)–C(1)–N(10)	117.0	116.6	116.5	C(12)–C(11)–N(10)–N(9)	21.0	57.6	57.6
C(1)–N(10)	1.441	1.436	1.436	C(11)–N(10)–N(9)	118.6	111.9	111.9	C(13)–C(12)–C(11)–N(10)	–53.0	–56.9	–56.9
N(9)–N(10)	1.510	1.519	1.519	C(12)–C(11)–N(10)	114.7	108.3	108.3	C(11)–C(12)–C(13)–C(14)[b]	65.6	0.1	0.1
C(11)–N(10)	1.473	1.459	1.459	C(11)–C(12)–C(13)	109.2	110.8	110.8	C(12)–C(13)–C(14)–N(9)[b]	–48.5	56.7	56.7
C(11)–C(12)	1.510	1.517	1.517	C(12)–C(13)–C(14)[b]	107.9	110.8	110.8	C(13)–C(14)–N(9)–N(10)[b]	17.4	–57.5	–57.5
C(12)–C(13)	1.510	1.534	1.534	C(13)–C(14)–N(9)[b]	116.8	108.3	108.3	C(11)–N(10)–N(9)–C(14)[b]	–2.8	–0.1	–0.1
C(13)–C(14)	1.514	1.517	1.517	C(14)–N(9)–N(10)	118.8	112.1	112.1				
C(14)–N(9)[b]	1.459	1.459	1.459								

[a] *R*-factor is 5.0%. For two groups of refined internuclear distances, the standard deviation 3σ of LS refinement was 0.010 Å. The bond angles were set equal to the theoretical MP2 values. The numbering of atoms is shown in Figure 1. [b] Ring closure parameters.

Table 2 Internuclear distances and angles for CH···N contacts.

Compound	$d_{C\cdots N}$/Å	$d_{H\cdots N}$/Å	∠C–H···N/deg	∠C–N–N/deg
bi-DABHx	3.578(2)	2.6175(16)	166.455(12)	93.06(4)
Ph-DABHp	3.684(2)	2.728(15)	160.7(12)	155.20(9)
ClPh-DABHp	3.672(3)	2.7434(17)	158.4(2)	150.47(18)
ClPh-DABHx[a]	3.640(2)/ 3.683(2)	2.778(16)/ 2.826(14)	151.8(11)/ 146.6(10)	93.83(8)/ 91.16(7)

[a] The unit cell contains two bicyclic fragments with different conformations. 3σ from the LS refinements are given in parentheses.

and all others. The bond angles were taken equal to the theoretical MP2 values. The final functions of the molecular intensity *sM*(*s*) and the radial distribution *f*(*r*) are shown in Figure 3, and the correlation matrix between the refined parameters is presented in Table S10.

The goodness of fit of the observed and calculated molecular intensity curves was primarily checked by running the KCED25 program without optimizing geometrical parameters and separately for all six conformers of the bi-DABHp molecule using MP2 estimates. The calculations showed that the agreement for conformers **a**, **b** and **d** is better than for the other conformers. The best agreement between the experimental and calculated molecular intensity was obtained for the final set of geometrical parameters given in Table 1 and a mixture of conformers **a**, **b** and a small amount of **d**.

The characteristic internuclear distances and bond angles of bi-DABHp are similar to those in the Ph-DABHp and ClPh-DABHp molecules, and the conformation of the bicyclic fragment in all three structures is almost the same. The bi-DABHp molecules form chains in the crystal along the *a* axis, linked by CH···N interactions, and the shortest contact with the nitrogen atom occurs through the H(1) atom (Figure 4). In the previously studied ClPh-DABHx, Ph-DABHp and ClPh-DABHp molecules with a similar bicyclic structure, the shortest C···N and, hence, H···N distances are noticeably larger than in the bi-DABHx compound (Table 2).

In the solid structure of bi-DABHp studied by XRD analysis† (Table S11), in addition to contacts between the CH group and nitrogen atoms, there are also other hydrogen contacts of the CH···N type (Tables S12–S17). They involve CH_2 groups closest to nitrogen atoms. The internuclear distances C···N in the case of the CH_2 group are greater than for the CH group: $d_{C(5)\cdots N(2)}$ = = 3.605(3), $d_{C(5)\cdots N(1)}$ = 3.758(2) and $d_{C(2)\cdots N(1)}$ = 3.917(3) Å. The strongest interactions are typical of the C(5)–H(5) contact, and, probably, there is bonding to both nitrogen atoms. In addition to chains along the *a* axis, the second CH_2 group, containing the C(2) atom of the bi-DABHp molecule, forms CH···N hydrogen bonds [$d_{C(2)\cdots N(1)}$ = = 3.6773(18) Å] with neighboring molecules in direction 110 (see Figure 4). Such intermolecular contacts are possible for both **b** and **d** conformers (see Figure 2), the total fraction of which in the gas phase is at least 67% according to estimates based on the relative Gibbs energies of the structures obtained at the DFT-D3 level. This fact can be considered as a confirmation that during

† *Crystal data for* bi-DABHp. $C_{10}H_{18}N_4$ (*M* = 194.28), triclinic, space group $P\bar{1}$ (no. 2), *a* = 4.317(3), *b* = 6.000(5) and *c* = 10.195(8) Å, α = 89.659(13)°, β = 86.252(13)°, γ = 74.001(12)°, *V* = 253.3(3) Å^3, *Z* = 1, d_{calc} = 1.274 g cm^{-3}, μ(MoKα) = 0.081 mm^{-1}, *T* = 120 K. Total of 1973 reflections were collected (4.004° ⩽ 2θ ⩽ 56.502°), 1240 unique (R_{int} = 0.0312, R_{sigma} = 0.0759) and used in the refinement. The final R_1 was 0.0589 [$I > 2\sigma(I)$] and wR_2 was 0.1380 (all data).

Single crystals of bi-DABHp were grown from acetone. A suitable crystal was selected and mounted on a glass needle in a Bruker APEX-II CCD diffractometer. The crystal was kept at 120 K during data collection. Using Olex2,[27] the structure was solved with the XS structure solution program[28] using direct methods and refined with the XL refinement package[28] using least squares minimization.

CCDC 2179110 contains the supplementary crystallographic data for this paper. These data can be obtained free of charge from The Cambridge Crystallographic Data Centre *via* http://www.ccdc.cam.ac.uk.

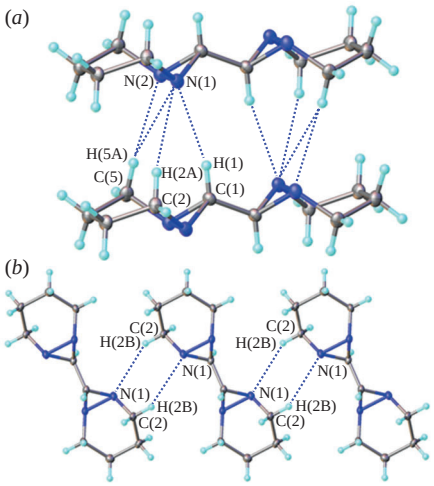

Figure 4 CH···N intermolecular contacts in the bi-DABHp solid structure, viewed along the (*a*) 100 and (*b*) 110 directions.

the evaporation (sublimation) of the substance, a not so significant change in conformation occurs.

Analysis of the 1D ^{1}H and ^{13}C NMR spectra of a solution of bi-DABHp in $CDCl_3$ (Figures S5 and S6) revealed that in solution the compound exists in only one conformation, since there are clear peaks of only one compound on a characteristic time scale of ~10^{-6}–10^{-1} s for NMR experiment.

For further validation, a set of 2D NMR spectra, namely ^{1}H–^{13}C HSQC (heteronuclear spectroscopy quantum correlation), ^{1}H–^{13}C HMBC (heteronuclear multiple bond correlation), ^{1}H–^{1}H COSY (correlation spectroscopy) and ^{1}H–^{1}H gNOESY (nuclear Overhauser effect spectroscopy), was recorded in a $CDCl_3$ solution at 298 K (Figures S7–S10), which makes it possible to assign the signals of all protons and carbon atoms and determine the relationship between them.

The ^{1}H–^{13}C HSQC and ^{1}H–^{13}C HMBC heteronuclear correlation NMR spectra were measured (Figures S7 and S8) and key parameters for unique atoms were extracted from these spectra (Tables 3 and S18). The data obtained show how far each proton is from a particular carbon atom, namely that they are separated by one, two or three bonds. The data illustrate the pairwise equivalence of atoms in two structural rings.

Combined data from the 2D ^{1}H–^{1}H COSY NMR spectrum (Figure S9) and 2D ^{1}H–^{1}H gNOESY NMR spectrum (Figures S10 and S11), which show the spatial arrangement of protons relative to each other, are listed in Table S19 and summarized in Table 4 only for unique atoms. These spectra show signals from protons separated by two or three bonds. As can be seen from the fragment of the ^{1}H–^{1}H gNOESY spectrum of bi-DABHp in $CDCl_3$ solution (see Figure S11), the H(15) proton has cross-peaks with the H(26) and H(32) protons, while the H(16) proton has cross-peaks with the H(18) and H(24) protons, which reflects the absolute similarity of the $CHN_2(CH_2)_2$ parts of the two rings, which can pass into each other as a result of inversion. Furthermore, cross-peaks reflect the arrangement of methylene group protons, which is possible only if the carbon–nitrogen skeleton has the form of a regular zigzag, which is present only in conformer **d** (see Figure 2).

Thus, a comprehensive investigation of the molecular structure of 1,1′,6,6′-tetraaza-7,7′-bi(bicyclo[4.1.0]heptane) (bi-DABHp) in the gas phase, carried out using electron diffraction, and in condensed phases using single-crystal X-ray diffraction and NMR spectroscopy in a $CDCl_3$ solution leads to the following conclusions.

Usually, when interpreting GED data, quantum chemical calculations are used to find the initial approximation for the key geometric parameters, which are subsequently refined, thereby speeding up the structural analysis. In this work, it turned out that the simulation

Table 3 ^{1}H–^{13}C HSQC and ^{1}H–^{13}C HMBC data for unique atoms in bi-DABHp.[a]

C atom	^{13}C NMR, δ/ppm	^{1}H–^{13}C HSQC interactions	^{1}H–^{13}C HMBC interactions	Equivalent atoms
C(1)	68.19	H(15)	H(16)/H(25)/H(26)/H(31)/H(32)	C(2)
C(5)	46.42	H(17)/H(18)	H(16)/H(19)/H(20)/H(21)/H(22)	C(14)/C(8)/C(11)
C(6)	16.66	H(19)/H(20)	H(17)/H(18)/H(21)/H(22)/H(23)/H(24)	C(7)/C(12)/C(13)

[a] The numbering of atoms is given in Figure 1.

Table 4 ^{1}H–^{1}H gNOESY and ^{1}H–^{1}H COSY data for unique atoms in bi-DABHp.[a]

H atom	^{1}H NMR, δ/ppm	Coupling constant, *J*/Hz	^{1}H–^{1}H gNOESY interactions	^{1}H–^{1}H COSY interactions
H(21)	1.55–1.61	–	H(19)/H(22)/H(23)	H(19)/H(20)/H(22)/H(23)/H(24)
H(22)	1.65–1.72	–	H(20)/H(21)/H(23)/H(24)	H(19)/H(20)/H(21)/H(23)/H(24)
H(15)	2.40	–	H(26)/H(32)	H(16)
H(18)	2.66–2.70	–	H(16)/H(17)/H(20)	H(17)/H(19)/H(20)
H(17)	3.38–3.41	12.0 [$^{2}J_{H(17)–H(18)}$], 8.1 [$^{3}J_{H(17)–H(19)}$]	H(18)/H(19)/H(20)	H(18)/H(19)/H(20)

[a] The numbering of atoms is given in Figure 1.

estimates are very close to the experimental structure; therefore, many parameters were fixed at the calculated values. The resulting mismatch factor R_f of the experimental and theoretical molecular intensity functions *sM*(*s*) is 5.0% and is in line with the accepted noise estimate in the GED experiment.

It was found that in the gas phase the bi-DABHp molecule exists mainly in the form of two conformers: in one, both seven-membered fragments are in the half-chair conformation, and in the other, one bicyclic fragment has the half-chair conformation, and the other is in the chair conformation. In the gas phase, a conformer with two chair-like bicyclic fragments is present in a small amount of ~11%. It is worth noting that while bi(bicyclo[4.1.0]-heptane) has a prevailing chair conformation, the six-membered hexahydropyridazine fragments prefer the boat conformation. This conformation is explained by the formation of intermolecular hydrogen bonds.

Analysis of the X-ray diffraction patterns of solid bi-DABHp and 1D and 2D ^{1}H and ^{13}C NMR spectra in $CDCl_3$ solution showed that in both condensed phases the compound exists in one conformation, structurally closest to conformer **d**, where both seven-membered fragments are in the half-chair conformation.

This work (by A.V.B., V.V.K., A.A.R. and I.F.S.) was supported by the Russian Foundation for Basic Research (project no. 20-03-00747A). XRD studies were performed with the support of the Ministry of Science and Higher Education of the Russian Federation using the equipment of Center for molecular composition studies of INEOS RAS.

Online Supplementary Materials

Supplementary data associated with this article can be found in the online version at doi: 10.1016/j.mencom.2023.01.030.

References

1 V. V. Kuznetsov, N. N. Makhova and M. O. Dekaprilevich, *Russ. Chem. Bull.*, 1999, **48**, 617.
2 V. V. Kuznetsov, S. A. Kutepov, N. N. Makhova, K. A. Lyssenko and D. E. Dmitriev, *Russ. Chem. Bull.*, 2003, **52**, 665.
3 E. G. Atavin, A. V. Golubinskii, M. V. Popik, V. V. Kuznetsov, N. N. Makhova and L. V. Vilkov, *J. Struct. Chem.*, 2003, **44**, 779 (*Zh. Strukt. Khim.*, 2003, **44**, 851).
4 I. I. Marochkin, E. P. Altova, V. V. Kuznetsov, A. N. Rykov and I. F. Shishkov, *Mendeleev Commun.*, 2022, **32**, 474.
5 V. V. Kuznetsov, I. I. Marochkin, A. S. Goloveshkin, N. N. Makhova and I. F. Shishkov, *Struct. Chem.*, 2017, **28**, 1211.
6 E. P. Altova, V. V. Kuznetsov, I. I. Marochkin, A. N. Rykov, N. N. Makhova and I. F. Shishkov, *Struct. Chem.*, 2018, **29**, 815.
7 I. I. Marochkin, V. V. Kuznetsov, Z. Li, A. N. Rykov, N. N. Makhova and I. F. Shishkov, *J. Mol. Struct.*, 2021, **1225**, 129066.
8 G. G. Ageev, A. N. Rykov, O. E. Grikina, I. F. Shishkov, I. V. Kochikov, V. V. Kuznetsov, N. N. Makhova and S. S. Bukalov, *Struct. Chem.*, 2022, **33**, 113.
9 A. P. Molchanov, D. I. Sipkin, Yu. B. Koptelov, J. Kopf and R. R. Kostikov, *Russ. J. Org. Chem.*, 2003, **39**, 1338 (*Zh. Org. Khim.*, 2003, **39**, 1410).
10 R. G. Kostyanovskii, G. V. Shustov, O. G. Nabiev, S. N. Denisenko, S. A. Sukhanova and E. F. Lavretskaya, *Pharm. Chem. J.*, 1986, **20**, 385 (*Khim.-Farm. Zh.*, 1986, **20**, 671).
11 A. Z. Baichurina, I. I. Semina and R. S. Garaev, *Bull. Exp. Biol. Med.*, 1996, **121**, 584 (*Byull. Eksp. Biol. Med.*, 1996, **121**, 648).
12 V. V. Kuznetsov, A. V. Shevtsov, M. I. Pleshchev, Yu. A. Strelenko and N. N. Makhova, *Mendeleev Commun.*, 2016, **26**, 391.
13 G. V. Shustov, G. K. Kadorkina, S. V. Varlamov, A. V. Kachanov, R. G. Kostyanovskii and A. Rauk, *J. Am. Chem. Soc.*, 1992, **114**, 1616.
14 M. Kamuf and O. Trapp, *Chirality*, 2011, **23**, 113.
15 M. I. Pleshchev, N. V. Das Gupta, V. V. Kuznetsov, I. V. Fedyanin, V. V. Kachala and N. N. Makhova, *Tetrahedron*, 2015, **71**, 9012.
16 A. O. Chagarovskiy, V. V. Kuznetsov, O. A. Ivanova, A. S. Goloveshkin, I. I. Levina, N. N. Makhova and I. V. Trushkov, *Eur. J. Org. Chem.*, 2019, 5475.
17 T. Sarkar, K. Talukdar, S. Roy and T. Punniyamurthy, *Chem. Commun.*, 2020, **56**, 3381.
18 H. Hu, J. Xu, F. Wang, S. Dong, X. Liu and X. Feng, *Org. Lett.*, 2020, **22**, 93.
19 A. P. Molchanov, M. M. Efremova, M. A. Kryukova and M. A. Kuznetsov, *Beilstein J. Org. Chem.*, 2020, **16**, 2679.
20 J. Cortes Vazquez, J. Davis, V. N. Nesterov, H. Wang and W. Luo, *Org. Lett.*, 2021, **23**, 3136.
21 D. V. Khakimov, L. L. Fershtat, T. S. Pivina and N. N. Makhova, *J. Phys. Chem. A*, 2021, **125**, 3920.
22 F. Neese, *Wiley Interdiscip. Rev.: Comput. Mol. Sci.*, 2012, **2**, 73.
23 M. J. Frisch, G. W. Trucks, H. B. Schlegel, G. E. Scuseria, M. A. Robb, J. R. Cheeseman, G. Scalmani, V. Barone, G. A. Petersson, H. Nakatsuji, X. Li, M. Caricato, A. V. Marenich, J. Bloino, B. G. Janesko, R. Gomperts, B. Mennucci, H. P. Hratchian, J. V. Ortiz, A. F. Izmaylov, J. L. Sonnenberg, D. Williams-Young, F. Ding, F. Lipparini, F. Egidi, J. Goings, B. Peng, A. Petrone, T. Henderson, D. Ranasinghe, V. G. Zakrzewski, J. Gao, N. Rega, G. Zheng, W. Liang, M. Hada, M. Ehara, K. Toyota, R. Fukuda, J. Hasegawa, M. Ishida, T. Nakajima, Y. Honda, O. Kitao, H. Nakai, T. Vreven, K. Throssell, J. A. Montgomery, Jr., J. E. Peralta, F. Ogliaro, M. J. Bearpark, J. J. Heyd, E. N. Brothers, K. N. Kudin, V. N. Staroverov, T. A. Keith, R. Kobayashi, J. Normand, K. Raghavachari, A. P. Rendell, J. C. Burant, S. S. Iyengar, J. Tomasi, M. Cossi, J. M. Millam, M. Klene, C. Adamo, R. Cammi, J. W. Ochterski, R. L. Martin, K. Morokuma, O. Farkas, J. B. Foresman and D. J. Fox, *Gaussian 16, Revision C.01*, Gaussian, Inc., Wallingford, CT, 2016.
24 V. A. Sipachev, *J. Mol. Struct.*, 2001, **567–568**, 67.
25 R. L. Hilderbrandt, *J. Chem. Phys.*, 1969, **51**, 1654.
26 B. Andersen, H. M. Seip, T. G. Strand, and R. Stolevik, *Acta Chem. Scand.*, 1969, **23**, 3224.
27 O. V. Dolomanov, L. J. Bourhis, R. J. Gildea, J. A. K. Howard and H. Puschmann, *J. Appl. Crystallogr.*, 2009, **42**, 339.
28 G. M. Sheldrick, *Acta Crystallogr., Sect. A: Found. Crystallogr.*, 2008, **64**, 112.

Received: 25th August 2022; Com. 22/6990